Theories and computer simulations of self-assembling surfactant solutions

1994 J. Phys.: Condens. Matter 6 6385

(http://iopscience.iop.org/0953-8984/6/32/003)

J. Phys.: Condens. Matter 6 (1994) 6385–6408. Printed in the UK

REVIEW ARTICLE

Theories and computer simulations of self-assembling surfactant solutions

Toshihiro Kawakatsu†¶, Kyozi Kawasaki†, Michihiro Furusaka‡, Hirofumi Okabayashi§ and Toshiji Kanaya‖

† Department of Physics, Faculty of Science, Kyushu University 33, Fukuoka 812, Japan
‡ BSF, National Laboratory for High Energy Physics, Tsukuba 305, Japan
§ Department of Applied Chemistry, Nagoya Institute of Technology, Nagoya 466, Japan
‖ The Institute for Chemical Research, Kyoto University, Uji 611, Japan

Received 26 April 1994

Abstract. We review recent theoretical and computer studies on formation and dynamics of self-assembled structures in surfactant solutions. One of the important features of surfactant solutions is the hierarchical nature in the structure, where atomic (microscopic), supermolecular (mesoscopic) and macroscopic structures coexist. In view of these structures with different length scales, many theoretical as well as computer models have been proposed from different points of view. We discuss relations between these models and give a brief review of our hybrid approach which is expected to bridge microscopic and macroscopic models.

1. Introduction

In recent condensed matter research, soft condensed materials, such as polymers, emulsions and colloidal suspensions, have become more and more popular as targets of theoretical as well as experimental studies. Considerable understanding of the static and dynamic properties of these materials has been achieved [1–3]. Theoretical developments have largely been driven by phenomenological modelling on the mesoscopic level [1], and moreover by the recent rapid developments in high-speed computers, the latter enabling us to perform large-scale numerical simulations of soft condensed materials. In this brief review, we discuss recent developments in the theoretical and computer investigations of dynamics of surfactant solutions as a typical example of the soft condensed materials research.

Surfactant is a material which is adsorbed onto interfaces (phase boundaries) and lowers the interfacial tension. A surfactant molecule has two distinct parts, which dissolve into different solvents, and therefore surfactant molecules are generally called amphiphiles. For example, a soap molecule has a hydrophilic part and a hydrophobic part; the former dissolves into water while the latter dissolves into oil. Thus the soap molecules are adsorbed onto water/oil interfaces and form two-dimensional sheets of soap molecules on the interfaces, where the soap molecules align with their hydrophilic parts directed to the water and their hydrophobic parts to the oil. Due to the in-plane pressure generated by such a surfactant sheet, the original interfacial tension of the water/oil interface is cancelled, leading to a

¶ To whom correspondence should be addressed. Permanent address: Department of Physics, Tokyo Metropolitan University, Hachioji, Tokyo 192–03, Japan.

0953-8984/94/326385+24$19.50

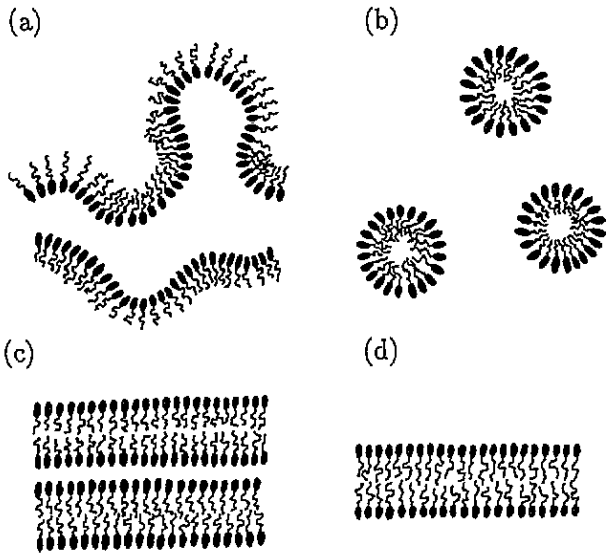

Figure 1. Schematic illustrations of typical domain structures formed in water/oil/surfactant three-component solutions. (a) Irregular bicontinuous, (b) micellar, (c) lamellar and (d) bilayer structures.

decrease in the effective interfacial tension. This is one of the most important roles of surfactants in solutions.

Depending on the composition of a water/oil/surfactant mixture, the system shows various complex domain structures [4]. In the low-surfactant-density region, it shows bicontinuous or micellar (globular) domain structures, while it shows regular arrangements of oil and water domains separated by surfactant sheets with lamellar, cylindrical or cubic symmetries in the high-surfactant-density region [4]. Several typical domain structures are schematically illustrated in figure 1. An important point is that these domain structures are in thermal equilibrium (i.e. they are thermodynamically stable). For a particular choice of the surfactant, the characteristic length of such domain structures can be of the order of 100–1000 Å, which is much larger than the molecular scale but is still below the macroscopic length scales. In contrast to the ordinary emulsions whose domain structure has a characteristic length on a macroscopic scale, these phases with microscopic domain structures are called *microemulsions*. On the other hand, when the surfactant molecules are dissolved into water, they form bilayer membranes upon self-assembling, which often take a closed shape called *a vesicle* [5] or sometimes take the form of an irregularly connected network of bilayers called *a sponge phase* [6].

In this brief review, we try to show an aspect of the current research on surfactant solutions focusing on the dynamics of formation processes of the self-assembled structures. We first give a brief overview of experimental results, in the next section. In section 3, various models to account for the static properties of microemulsions are summarized. We will see that most of the existing theories and computer simulations are done either on the microscopic level or on the macroscopic level and a gap seems to exist between these two kinds of approach. In section 4, we explain the relations between microscopic and macroscopic models with the use of a coarse-graining procedure within the mean-field approximation. We also explain the hybrid approach to microemulsion dynamics,

which is expected to bridge the gap between microscopic and macroscopic approaches. Theoretical and computer-simulation results of several models are presented in section 5. *Section 6 is devoted to discussion.*

2. Some experimental results

Experimental investigations on structures of microemulsions have been performed with the light and neutron scattering techniques and with the electron micrograph technique combined with the freeze-fracture method [7]. Most of these works are focused on the static or equilibrium structures of microemulsions.

2.1. Equilibrium domain structures

It is well known that a water/oil/surfactant mixture shows irregular bicontinuous domain structures or irregularly arranged micellar domain structures when the surfactant density is relatively low [4] (see figure 1). Structures of microemulsions can directly be observed with the freeze-fracture electron micrograph technique [8], by which one recognizes that a characteristic periodicity exists in the domain configuration although the domains are not arranged like a perfect crystal. Such a periodicity is understood as the origin of the scattering peak from microemulsions observed by light and neutron scattering [9]. In figure 2, typical scattering intensities from a microemulsion are shown, where a single remarkable peak appears [10]. A similar scattering peak can also be seen in the scattering intensity from binary polymer mixtures which undergo spinodal decomposition [11]. In the case of spinodally decomposing binary mixtures, the position of the scattering peak gradually shifts to the lower-wave-number side, and therefore there is no equilibrium scattering peak with a finite wave number.

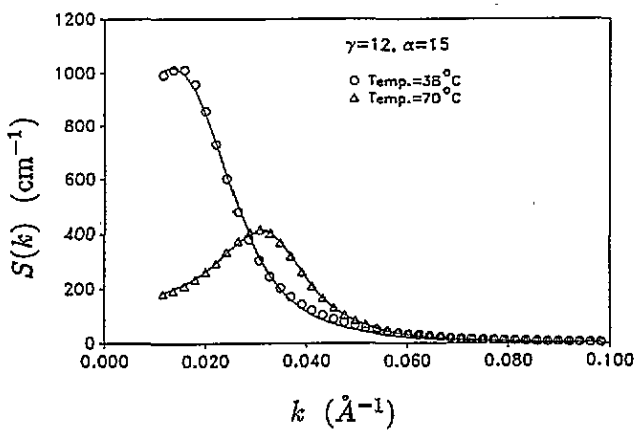

Figure 2. Typical scattering intensity profiles obtained by small-angle neutron scattering experiments on water/*n*-decane/AOT mixture with 15% oil weight fraction and 12% AOT weight fraction (see [10]).

On the other hand, in the case of binary mixtures containing surfactants, a stationary scattering peak with a finite wave number does exist even in the equilibrium state as is

shown in figure 2. Such a difference originates from the very low interfacial tension of the surfactant-adsorbed interfaces. When an interface has non-vanishing interfacial tension, there is an excess free energy at interfaces, which amounts to the interfacial tension multiplied by the interfacial area. As the interfaces are driven in such a way that this interfacial excess free energy is reduced, the total interfacial area decreases in time and the coarsening of the domains proceeds. Such a driving force for the interfaces is greatly reduced when a surfactant is dissolved into the binary mixture. This is the origin of the stable scattering peak from microemulsions. A brief explanation of this problem is given in subsection 5.2.

2.2. *Dynamics of phase separation*

When a water/oil/surfactant mixture is used as a specimen for scattering experiments, it is difficult to study dynamics of formation processes of the final domain structure because of the very short time scale of the phase separation as in a normal binary fluid mixture [12], which is beyond the resolution of time-resolved light/neutron scattering experiments. However, use of polymer systems enables us to observe temporal evolution of the phase separation due to the slow dynamics of polymers caused by the entanglements between polymer chains. A block copolymer is a kind of surfactant, which possesses amphiphilic nature. A linear diblock copolymer chain consists of two distinct subchains connected at one end as is shown schematically in figure 3. For example, if we consider an A–B diblock copolymer dissolved into an A/B binary homopolymer blend which undergoes phase separation, the A subchain dissolves into the phase with a high concentration of the A homopolymers (A-rich phase), while the B subchain dissolves into the B-rich phase. Thus the A–B block copolymer serves as a surfactant in the A/B homopolymer blend. A binary polymer blend containing an amphiphilic block copolymer shows similar phase-separated structures to microemulsions.

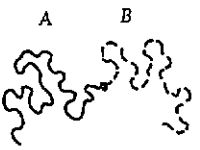

Figure 3. A schematic illustration of an A–B diblock copolymer chain.

In studying the phase-separation dynamics by scattering experiments, there are several useful observable quantities, which can be compared with theoretical predictions. The scattering function $S(k,t)$ and the characteristic length $l(t)$ are such useful observables. The scattering function (or scattering intensity) $S(k,t)$ for isotropic phases is given by

$$S(k,t) \equiv \int \mathrm{d}\boldsymbol{r} \exp(-\mathrm{i}\boldsymbol{k}\cdot\boldsymbol{r})\langle X(\boldsymbol{r},t)X(\boldsymbol{0},t)\rangle \tag{2.1}$$

where $k \equiv |\boldsymbol{k}|$ is the magnitude of the wavevector $\boldsymbol{k}$, $X(\boldsymbol{r},t)$ is the concentration difference between the two components of the binary mixture at position $\boldsymbol{r}$ at time t and $\langle\ \rangle$ denotes the thermal average. The characteristic length $l(t)$ is the measure of the average domain size and is often defined as the inverse of the characteristic wave number $\bar{k}$ defined for example by the first moment of $S(k,t)$ or by the wave number for which $S(k,t)$ takes its maximum value. These quantities can be calculated from theoretical models and from computer simulations. Therefore, experimental data for these quantities are important to check the validity of theoretical models.

Scattering experiments on the dynamics of phase separation in polymer/block copolymer systems have just started recently [13, 14]. Roe and co-workers investigated the dynamics of formation processes of micellar structures of a polystyrene/polybutadiene/stylene-butadiene diblock copolymer three-component polymer mixture with the light scattering and optical microscopic techniques [13]. They investigated the growth law of the characteristic length which shows that

$$l(t) = \alpha t^z \tag{2.2}$$

where t is time, α is a proportionality factor and z is the growth exponent. The power law growth given by equation (2.2) is known as dynamical scaling [15]. They observed the same growth exponent for binary polymer mixtures both without and with the block copolymer. The only difference they found is a reduction in the prefactor α when the block copolymer is added to the polymer blend.

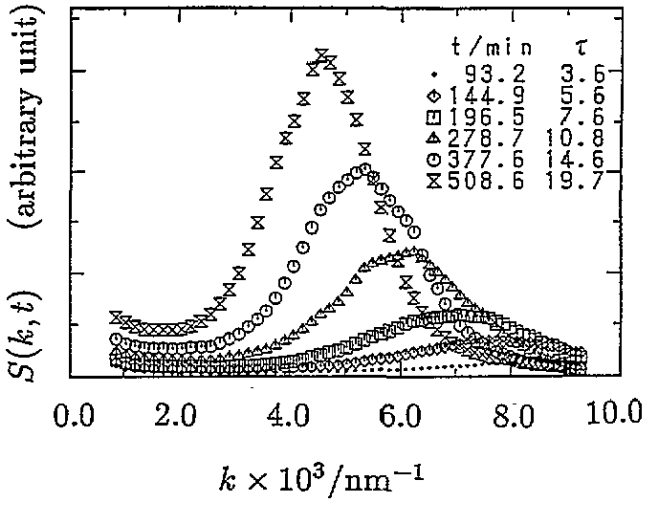

Figure 4. Temporal evolution of the scattering intensity $S(k, t)$ observed in a light scattering experiment on a polymer blend containing 6% block copolymer. t is the real time and τ is a dimensionless time measured in units of the characteristic time in the early stage of the spinodal decomposition (see [14]).

Hashimoto and Izumitani performed light scattering experiments using polybutadiene (PB)/stylene-butadiene random copolymer (SBR)/SBR–PB diblock copolymer (SBR-b-PB) [14]. Their experiments were done at the critical quench, where the volume fractions of the PB phase and that of the SBR phase are almost equal and therefore a bicontinuous domain structure is formed. The growth law equation (2.2) and other dynamical scaling properties were examined and the results are shown in figures 4–6. Figure 4 shows the temporal change of the scattering intensity $S(k, t)$, where one can clearly observe that the peak shifts to the lower-wave-number side as time goes on, which is a sign of the coarsening of domains. The temporal evolution of the wave number at the peak position of $S(k, t)$ is shown in figure 5, from which one can determine the growth exponent z in equation (2.2). One observes a decrease in the growth exponent z in a sufficiently late stage of the phase separation due to

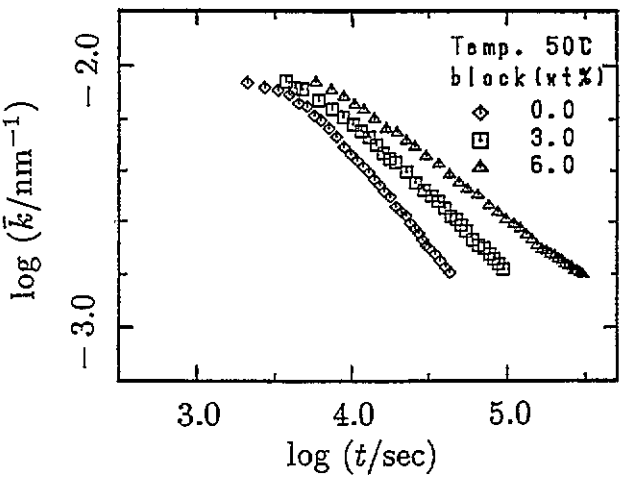

Figure 5. Experimentally observed temporal evolution of the characteristic wave number $\bar{k}$ defined as the peak position of $S(k, t)$ on a double logarithmic scale. Weight fractions of the block copolymer are 0%, 3% and 6%, respectively (see [14]).

the added block copolymer. Izumitani and Hashimoto also investigated the functional form of the scattering function $S(k, t)$. In figure 6, the scaled scattering function $\tilde{S}(x)$ defined as

$$S(k, t) = \bar{k}^{-d}\tilde{S}(k/\bar{k}) \tag{2.3}$$

for the cases without and with added block copolymer are shown. The scattering function does not change its functional form appreciably in spite of the obvious slowing down of the domain growth.

In the following sections, we show how to model and analyse theoretically such dynamical processes.

3. Theoretical models—brief overview

As for the experimental situation, theoretical developments in the understanding of microemulsions have been achieved mainly for the equilibrium properties, such as the calculation of the phase diagram of three-component mixtures or the statistics of equilibrium domain configurations. In this section, we give a brief overview of models of microemulsions for later convenience. For a complete review of theories on static properties, readers may refer to the recent article by Gompper and Schick [16].

3.1. Interface models

Theoretical studies of equilibrium domain configurations in microemulsions have been initiated by the pioneering work by Schulman and Montagne [17] and later works by Talmon and Prager [18], by de Gennes and Taupin [19] and by Widom [20]: Here we summarize Widom's model [20], which has a rather simple form but retains essential features of microemulsions. Widom used a cubic lattice with a lattice constant ξ to specify positions of water-rich domains, oil-rich domains and surfactant. The lattice constant ξ is regarded

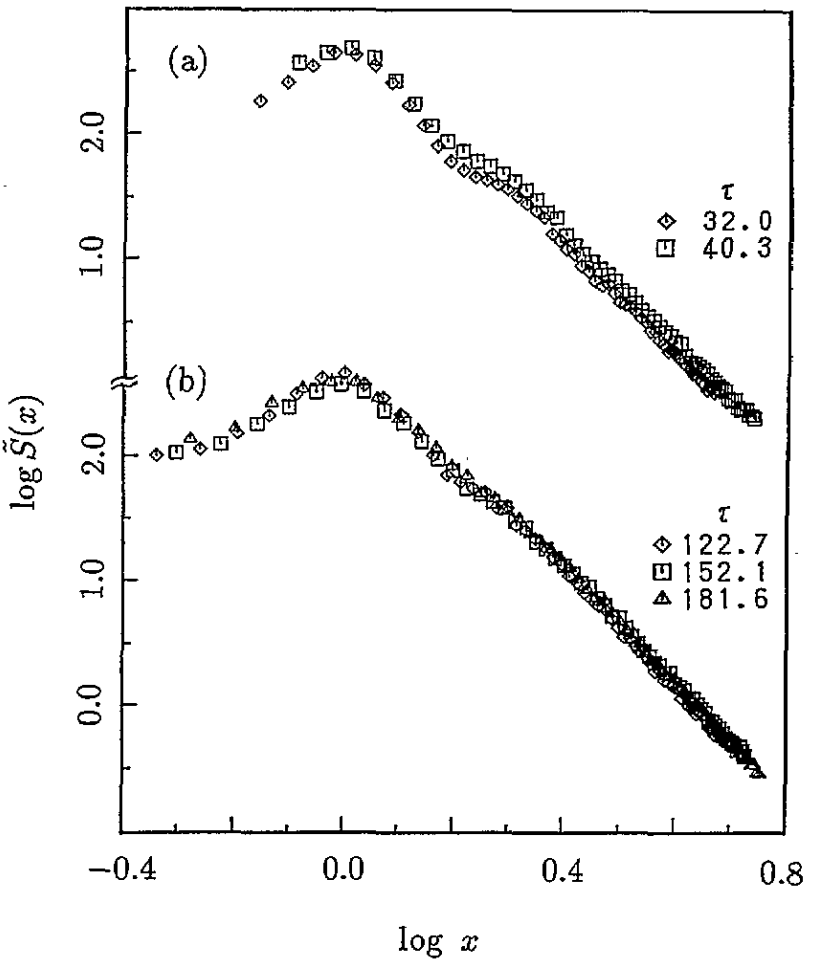

Figure 6. Experimentally observed scaled scattering functions $\tilde{S}(x)$ defined by equation (2.3). The block copolymer content is (a) 0% and (b) 6%, respectively, and τ is the dimensionless time (see [14]).

as the correlation length of the composition fluctuation, over which the relative composition between water and oil can be regarded as almost constant. Thus each cubic cell on each lattice point is filled with either only water or only oil. The surfactant is assumed to lie on the faces between water-rich cells and oil-rich cells, and therefore the total area of faces separating water-rich cells and oil-rich cells is proportional to the surfactant density. Assuming that the water-rich cells and oil-rich cells are distributed randomly on the lattice (mean field approximation), the total free energy of the system can be expressed in terms of the volume fractions of water, oil and surfactant denoted as ϕ_A, ϕ_B and ρ_S and of the correlation length ξ [20]:

$$F = \mu_A\phi_A + \mu_B\phi_B + k_BT(\phi_A \ln\phi_A + \phi_B \ln\phi_B) + 6\sigma_0\phi_A\phi_B/\xi \\ - k_BT\rho_S \ln(\Sigma/\Sigma_0) + D\rho_S[1 - \Lambda(\phi_A - \phi_B)\xi]/2\xi^2 \qquad (3.1)$$

where μ_A and μ_B are the chemical potentials of water and oil, σ_0 is the bare interfacial tension of the water/oil interface, Σ is the total area of the water/oil interface which is a

function of ϕ_A, ϕ_B and ξ, and Σ_0, D and Λ are constants. The first line is the free energy of the water/oil binary mixture, the first and the second terms in the second line are the free energy of the two-dimensional surfactant fluid and the bending energy of surfactant-adsorbed interfaces, respectively. The equilibrium phase diagram can be obtained by minimizing F with respect to ξ for the given volume fractions ϕ_A, ϕ_B and ρ_S. The calculated phase diagram was found to reproduce the essential features of the real phase diagram [4, 20]. A similar approach was later used to reproduce scattering functions from microemulsions [21]. Note that the treatment adopted here is not a microscopic approach but a coarse-grained mesoscopic approach, because the lattice constant ξ is usually much larger than the atomic length scale, where each lattice point corresponds to a group of molecules rather than a single molecule. Such a description was adopted in order to describe the mesoscopic structure of microemulsions effectively by averaging out the microscopic details of water/oil/surfactant molecules.

3.2. Lattice models

Besides the interface models mentioned in the preceding subsection, other microscopic spin–lattice models have been proposed as models of microemulsions. The lattice model of microemulsions proposed by Widom [22] is the origin of a diverse number of lattice models of microemulsions used in the later analytical studies and computer simulations [23–28]. In Widom's lattice model, water, oil and surfactant molecules are described by nearest-neighbour A–A, B–B and A–B pairs, respectively (see figure 7 for a schematic explanation).

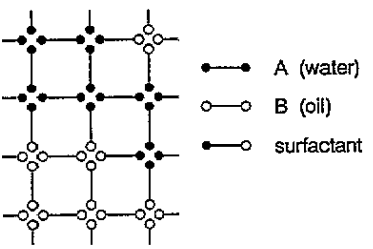

Figure 7. A schematic illustration of Widom's spin–lattice model of a microemulsion.

Lattice models can also be extended in such a way that the internal degrees of freedom of constituent molecules are taken into account. Larson and co-workers used a lattice model to study molecular configurations in microemulsions [28]. In their model, the water molecule is modelled as a monomer which occupies a single lattice point, while the oil molecule is modelled as a short linear chain consisting of the same monomer units which occupy consecutive lattice points. The surfactant molecule is modelled as a linear chain consisting of several water-like (A) units and oil-like (B) units. Here, each lattice point (or monomer) is regarded as a microscopic object. The system has only one interaction parameter χ defined by $\chi \equiv \chi_{AB} - (\chi_{AA} + \chi_{BB})/2$, where χ_{AA}, χ_{BB} and χ_{AB} are the interaction energies between A–A, B–B and A–B nearest-neighbour pairs divided by k_BT. Using the Monte Carlo (MC) simulation technique, Larson *et al* succeeded in reproducing various equilibrium domain configurations [28]. A configuration generated by the MC simulation on a two-dimensional system is shown in figure 8. Here, the interaction parameter χ is chosen as $\chi = 0.5$ so that the water units and oil units are repelling each other and the surfactant chain is composed of

four water units and four oil units. Although the surfactant molecules align on the water/oil interfaces, the configuration of the surfactant molecules in the layer is random rather than a regularly aligned monolayer as is often sketched in schematic pictures.

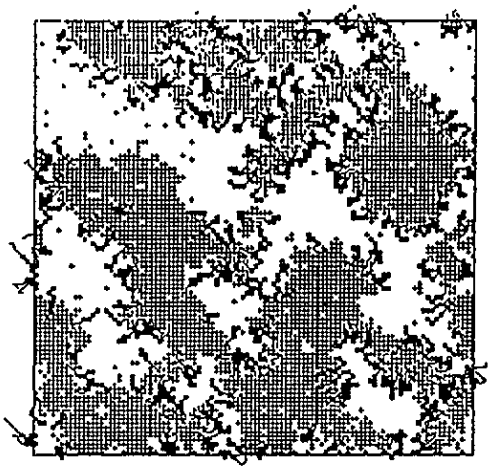

Figure 8. A snapshot pictures of a model microemulsion by Larson and co-workers (see [28]).

3.3. Molecular models

Another microscopic approach is based on a fully molecular point of view. Smit and co-workers used a similar modelling to that used by Larson *et al* but without assuming the underlying lattice [29]. In this model, the water molecule and the oil molecule are modelled as spherical monomers of different kinds interacting via the truncated Lennard-Jones (LJ) potential:

$$U_{ij}(r) = \begin{cases} \phi(r) - \phi(R_{ij}^c) & r \leqslant R_{ij}^c \\ 0 & r > R_{ij}^c \end{cases} \qquad (i, j = \text{water or oil}) \tag{3.2}$$

where R_{ij}^c is the cut-off distance of the interaction between the i–j pair and $\phi(r)$ is the so-called LJ potential defined as

$$\phi(r) = 4\epsilon\left[\left(\frac{\sigma}{r}\right)^{12} - \left(\frac{\sigma}{r}\right)^{6}\right] \tag{3.3}$$

where ϵ and σ are the energy unit and the interaction diameter respectively. The cut-off distance is taken to be $R_{ww}^c = R_{oo}^c = 2.5\sigma$ and $R_{wo}^c = 2^{1/6}\sigma$ (w and o stand for water and oil) so that the interaction between oil and water is purely repulsive while the interaction between water–water and oil–oil pairs includes the attractive part of the LJ potential. This selection of the cut-off distances causes the water/oil mixture to phase separate. The surfactant molecule is modelled as a linear chain of water monomers and oil monomers. Using the molecular dynamics (MD) simulation technique, equilibrium configurations are generated.

Such a molecular model combined with the MD simulation technique can also be used to investigate dynamical properties of microemulsions. Laradji *et al* performed a molecular dynamics simulation on the phase separation processes of a three-component mixture of A/B/surfactant [30]. In their simulation, the A and the B molecules are modelled by spheres

interacting via modified Lennard-Jones potentials and the surfactant molecule is modelled by a pair of an A molecule and a B molecule connected by a harmonic spring. They performed a large-scale simulation and showed that their model can reproduce essential features of the phase-separating binary mixtures containing surfactants, such as the slowing down of the phase separation in the late stage and the final domain structures. Such an MD simulation requires a long computer time because one has to treat all the molecular degrees of freedom of the three-component mixture. In order to construct a more economical model, a reduction of the degrees of freedom is necessary.

3.4. Continuum models

So far, we have reviewed the models where the microemulsion is described by discrete variables like lattice points or discrete monomers. As is well known in the field of critical phenomena [31], discrete models can be mapped, under certain conditions, to continuum models where the system is described by continuous field variables such as the density distributions or the relative concentration of binary mixtures. Such a mapping is performed by coarse graining the system and retaining only the slowly varying and long-wavelength variables. Instead of deriving the coarse-grained free energy from a microscopic model, an explicit expression for the coarse-grained free-energy functional can also be obtained by pure symmetry arguments on the macroscopic level. This is done by expanding the free-energy functional in power series of the continuous field variables and by retaining the leading several relevant terms with the same symmetry properties as those of the system itself.

Such continuum models have successfully been used to investigate critical phenomena like phase separation of binary mixtures or order–disorder phase transitions [31]. Extensions of the theory to surfactant solutions were made only recently [32–35]. Here, we show the model proposed by Laradji *et al* for a binary mixture containing a surfactant [34]. In their model, two continuous fields are used to describe the local phase separation of the water/oil binary mixture and the local concentration of the surfactant. The phase separation of the water/oil mixture is described by a scalar field $X(r) \equiv \phi_A(r) - \phi_B(r)$, where $\phi_A(r)$ and $\phi_B(r)$ are local densities of water and oil, respectively. On the other hand, the local density of surfactant is described by another scalar field $\rho_S(r)$. The free-energy functional is assumed to have the following form:

$$F = \int dr\ [c(\nabla X)^2 - rX^2 + uX^4 + g\rho_S^2 X^2 + a\rho_S^2 - \mu\rho_S - s\rho_S(\nabla X)^2] \tag{3.4}$$

where c, r, u, g, a, μ and s are phenomenological parameters and are all positive. The surface-active effect of surfactant is expressed by the last term, which expresses two major properties of surfactant. One is the tendency that the surfactant is adsorbed to the interfacial region of the binary mixture where $(\nabla X)^2$ is large. The other important surfactant property is the reduction of the interfacial tension. As the surfactant is adsorbed to the interfacial region more and more, the total coefficient of $(\nabla X)^2$ in equation (3.4) is reduced. As the square of the interfacial tension of the model equation (3.4) is proportional to the coefficient of $(\nabla X)^2$, the interfacial tension is reduced by the surfactant adsorption onto the interface.

4. From microscopic to macroscopic—reduction of degrees of freedom

In the preceding section, we reviewed existing theoretical models proposed from different points of view. These models are classified roughly into two categories. One is the

microscopic models such as the molecular models and lattice models, where both the surfactant and the solvent are treated as discrete degrees of freedom. The other group is the macroscopic models like the continuum models using long-wavelength fluctuations in compositions and surfactant orientation in order to describe the total free energy of the system. Interface models can also be categorized into these macroscopic models, because a coarse-grained picture is adopted to model the domain structures and surfactant sheets. No model exists between these two groups.

Macroscopic models should in principle be derived from the microscopic models by coarse graining the microscopic degrees of freedom and projecting such microscopic degrees of freedom onto several slow and long-wavelength modes. Here we consider such a procedure to relate the microscopic models and macroscopic models. One point which should be noted is the fact that there are several length scales coexisting in the surfactant solutions. The smallest scale is the molecular size of the solvent. (We are not interested in the phenomena on the submolecular levels.) The size of the surfactant molecule is in general different from that of the solvent molecule. For example, if a block copolymer is used as a surfactant, the size of the surfactant molecule can be much larger than the solvent molecules. Another length scale is the correlation length in the composition fluctuation of the phase separating binary solvent, which can be much larger than the molecular size of the solvent when the system is close to the critical point. The largest intrinsic length scale will be the average size of the domains separated by surfactant sheets. The macroscopic models obtained as a result of the coarse-graining procedure include these characteristic lengths explicitly/implicitly in the model parameters.

Now, we discuss how a macroscopic model can be derived from a simple microscopic model. We will discuss this within the mean field approximation with the simple continuum approximation of the long-wavelength fluctuations. For a more rigorous treatment for the model parameters, one should rely on the renormalization group method [36]. As a starting point, we adopt a lattice model of an A/B binary solvent containing a surfactant. An A or a B solvent molecule is assumed to occupy a single lattice point, and the surfactant molecule is described by a diblock copolymer of $N = N_A + N_B$ monomers composed of a linear chain of N_A molecules (monomers) of the A solvent and a chain of N_B molecules (monomers) of the B solvent. The total free energy of the system divided by $k_B T$, denoted as F, is composed of three contributions:

$$F = E - S_t - S_{int} \tag{4.1}$$

where E is the interaction energy between monomers, S_t is the entropy associated with the translational degrees of freedom of molecules and S_{int} is the entropy associated with the internal degrees of freedom of the surfactant molecules. The local mean field approximation leads to the following explicit expressions for E and S_t up to the lowest relevant order apart from irrelevant constant contributions:

$$E = \frac{1}{2\rho_0}\int dr\ [\bar{z}\{\chi_{AA}\rho_A^2 + \chi_{BB}\rho_B^2 + 2\chi_{AB}\rho_A\rho_B\} - a^2\{\chi_{AA}(\nabla\rho_A)^2 + \chi_{BB}(\nabla\rho_B)^2 + 2\chi_{AB}\nabla\rho_A \cdot \nabla\rho_B\}] \tag{4.2}$$

$$S_t = -\int dr\left[\phi_A \ln\phi_A + \phi_B \ln\phi_B + \frac{(\psi_A + \psi_B)}{N}\ln(\psi_A + \psi_B)\right] \tag{4.3}$$

where a is the lattice spacing, $\rho_0 \equiv 1/a^3$ is the total monomer number density, $\bar{z}$ is the number of nearest-neighbour lattice points ($\bar{z} = 6$ for a cubic lattice), $\phi_K(r)$ and $\psi_K(r)$ (K = A or B) are the local monomer number densities of the K component of the solvent and of the

surfactant, respectively, $\rho_K(r) \equiv \phi_K(r) + \psi_K(r)$ is the number density of the K monomers including both the solvent and the surfactant and $\chi_{KK'}$ is the interaction energy of a K–K′ monomer pair divided by k_BT. The expression for S_{int} depends on the polymerization index N of the surfactant molecule and will be considered separately.

Introducing the order parameters $X(r)$ and $Y(r)$ by

$$X(r) \equiv \phi_A(r) - \phi_B(r) \qquad Y(r) \equiv \psi_A(r) - \psi_B(r) \tag{4.4}$$

the free-energy expression F is rewritten using equations (4.1)-(4.3) as

$$F = \frac{1}{2\rho_0}\int dr\left[-\frac{\chi\bar{z}}{2}(X+Y)^2 + \frac{\chi a^2}{2}\{\nabla(X+Y)\}^2 + \rho_0\{(\phi+X)\ln(\phi+X) + (\phi-X)\ln(\phi-X) + \frac{2\psi}{N}\ln\psi\}\right] + S_{int} \tag{4.5}$$

where $\phi(r) \equiv \phi_A(r) + \phi_B(r)$ and $\psi(r) \equiv \psi_A(r) + \psi_B(r)$, respectively, and $\chi \equiv \chi_{AB} - (\chi_{AA} + \chi_{BB})/2$ is the usual χ parameter. In equation (4.5) we omitted some constant contributions to the free energy using the fact that the order parameters X, Y, ϕ and ψ are macroscopic density fields which are conserved variables. The equations of motion for these conserved order parameters take the form of the continuity equation, for example

$$\frac{\partial}{\partial t}X(r,t) = -\nabla \cdot j_X(r,t). \tag{4.6}$$

In the purely dissipative case, the current j_X is derived from the thermodynamic chemical potentials as

$$j_X = -L^{XX}\nabla\mu_X - L^{XY}\nabla\mu_Y - L^{X\psi}\nabla\mu_\psi \tag{4.7}$$

where $\mu_X \equiv \delta F/\delta X$ etc. Here, we have used the fact that only X, Y and ψ are independent variables due to the condition $\phi(r) + \psi(r) = \rho_0$ (= constant). Similar equations hold also for Y and ψ, where the Onsager kinetic coefficients $L^{\alpha\beta}$ etc satisfy $L^{\alpha\beta} = L^{\beta\alpha}$.

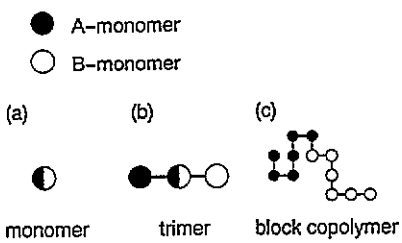

Figure 9. Model surfactant molecules on a cubic lattice. (a) monomeric surfactant, (b) trimeric surfactant and (c) polymeric surfactant, respectively.

Equations (4.5)–(4.7) describe the dynamics of slow and long-wavelength fluctuations of the system. In the following, we derive explicit expressions of the equations of motion for several particular models illustrated in figure 9, i.e. (a) monomeric surfactant, (b) trimeric surfactant and (c) polymeric surfactant. In the following, we limit our discussions to the case with the equimolar composition of A and B species for simplicity.

4.1. Monomeric surfactant—impurity molecule

As an example of small surfactant molecules, let us consider a monomer made of one half of an A monomer and one half of a B monomer connected rigidly, which occupies a single lattice point (i.e. $N = 1$, see figure 9(a)). Noting the fact that $Y \equiv 0$ and $S_{\text{int}} = 0$, equation (4.5) can be reduced to

$$F = \frac{1}{2\rho_0}\int \mathrm{d}r\Big[-\frac{\chi\bar{z}}{2}X^2 + \frac{\chi a^2}{2}(\nabla X)^2 + \rho_0\{(\phi+X)\ln(\phi+X) + (\phi-X)\ln(\phi-X) + 2\psi\ln\psi\}\Big]. \tag{4.8}$$

In this monomeric surfactant case, the amphiphilic nature, which is the most important feature of surfactants, is not taken into account explicitly. Therefore, the surfactant molecule in this case is just like an impurity molecule.

4.2. Trimeric surfactant—small surfactant molecule

The simplest way to mimic the amphiphilic property will be to use a dimer composed of an A monomer and a B monomer [37], or to use a rigid linear trimer molecule composed of an A monomer, an O monomer and a B monomer [25], where the O monomer is the neutral monomer introduced in the preceding subsection. In this case, let us introduce [38, 39]

$$\rho_{\text{S}}(r) \equiv \sum_i \delta(r - r_i) \tag{4.9a}$$

$$s(r) \equiv \sum_i \hat{s}_i\delta(r - r_i) \tag{4.9b}$$

and

$$S(r) \equiv \sum_i \hat{s}_i\hat{s}_i\delta(r - r_i) - \frac{1}{3}\rho_{\text{S}}(r)\mathbf{1} \tag{4.9c}$$

where r_i is the position of the centre monomer of the ith surfactant molecule, $\hat{s}_i$ is the unit vector from the B monomer to the A monomer of the ith surfactant molecule and $\mathbf{1}$ is the unit tensor. Note that, when N is small, $\rho_{\text{S}}(r)$ is approximately related to $\psi(r)$ by $\rho_{\text{S}}(r) \sim \psi(r)/N$ by its definition. Using these definitions, the free energy can be rewritten up to the lowest relevant order as equation (4.1) with

$$E = \frac{\chi}{\rho_0}\int \mathrm{d}r\ \left[-\frac{\bar{z}}{4}X^2 + \frac{a^2}{4}(\nabla X)^2 - \bar{z}as\cdot\nabla X - \bar{z}a^2(\nabla\cdot s)^2\right] \tag{4.10a}$$

$$S_{\text{t}} = -\frac{1}{2}\int \mathrm{d}r\ [(\phi+X)\ln(\phi+X) + (\phi-X)\ln(\phi-X) + 2\rho_{\text{S}}\ln\rho_{\text{S}} + 2a^2(\ln\rho_{\text{S}})\nabla\nabla : S] \tag{4.10b}$$

and

$$S_{\text{int}} = -\frac{3}{2}\int \mathrm{d}r\ \rho_{\text{S}}\left[\left(\frac{s}{\rho_{\text{S}}}\right)^2 + \text{Tr}\left(\frac{S\cdot S}{\rho_{\text{S}}^2}\right)\right] \tag{4.10c}$$

where S_{int} is the entropy of the directional degrees of freedom of the surfactant molecules and Tr denotes the trace of the tensor. In this model, the order parameter $Y(r)$, the density difference between the A monomers and B monomers of the surfactant, is expressed in terms of an vector field $s(r)$ and a tensor field $S(r)$ reflecting the fact that an A monomer and a B monomer are connected by a short rigid bond and cannot undergo macro phase separation just like the microphase separating block copolymer melts [40–43].

The model free energy, equations (4.10*a–c*), contains most of the important terms in the model proposed by Chen *et al* [32], where only the local density difference $X(r)$ and the local orientation of surfactant molecules $s(r)$ are taken into account.

As we retained only terms up to second order in ρ_s and S in equations (4.10*a–c*), these variables can be eliminated by integrating them out. Neglecting the contributions from spatial derivatives of higher order than second order, the free-energy functional becomes

$$F = \frac{1}{2\rho_0}\int \mathrm{d}r \left[-\frac{\bar{z}\chi}{2}X^2 + \left(\frac{a^2\chi}{2} - \frac{(a\bar{z}\chi)^2}{3\rho_0}\rho_S\right)(\nabla X)^2 + \rho_0\left\{(\phi + X)\ln(\phi + X) + (\phi - X)\ln(\phi - X) + 2\rho_S \ln \rho_S + \frac{2a^2}{9}\rho_S \nabla^2 \ln \rho_S\right\}\right]. \tag{4.11}$$

By expanding the second and the third lines of equation (4.11) in power series of small fluctuations in ϕ, ρ_S and X around their average values, one can confirm that equation (4.11) is essentially the same as that used by Laradji *et al* [34] except for small differences.

4.3. Polymeric surfactant—large surfactant molecule

When the surfactant molecule is a block copolymer with a large polymerization index ($N \gg 1$), the surfactant molecule can be regarded as a mesoscopic object just like a cloud of monomers distributed over the range of R_G, where R_G is the radius of gyration of the block copolymer chain [1]. This R_G can be as large as the correlation length ξ in the composition fluctuation of the binary mixture, the latter being the length scale over which the averaging procedure for the coarse graining is performed. For example, the local composition $X(r)$ should be regarded as a variable whose short-wavelength fluctuations below ξ have already been averaged out. Therefore, if the size of the surfactant molecule R_G is of the same order as ξ, the treatments of the surfactant in sections 4.1 and 4.2 are not appropriate, and one has to take the spatial extent of the surfactant molecules into account.

One way to accomplish this is to adopt the results of the recent density-functional theories of block copolymer melts [40–43]. For example, Ohta and Kawasaki studied the strong-segregation limit of a block copolymer melt by splitting the free-energy functional into two parts [42]. One is the short-range interaction which originates from the local monomer–monomer interaction. This short-range interaction F_{SR} takes the same form as that for the order parameter $X(r)$ in equations (4.2) and (4.3). The other is the long range interaction due to the polymer nature. As the A subchain and the B subchain are connected by a chemical bond, they cannot undergo macrophase separation. Thus the composition fluctuation of the block copolymer should vanish in the limit $k \to 0$, where k is the wave number. Such a penalty is accounted for by adding an extra interaction:

$$F_{LR} = \frac{\kappa}{2}\int \mathrm{d}r\ G(r - r')Y(r)Y(r') \tag{4.12}$$

where κ is a coefficient which depends on N as $\kappa \sim N^{-2}$ and $G(r - r')$ is the Green function for the diffusion field defined by $\nabla^2 G(r - r') = -\delta(r - r')$ [42, 43]. Replacing the surfactant parts in equations (4.1)–(4.3) by these F_{SR} and F_{LR}, one obtains a total free energy for solvent/block copolymer mixtures, which can be used as a suitable model for studying the dynamics of phase separations [44].

4.4. Hybrid model

In the model discussed in section 4.3, block copolymer chains are described by continuous fields $Y(r)$ and $\psi(r)$. Thus the details of individual surfactant molecules such as the molecular shape, have already been averaged out. However, when the surfactant molecule is a macromolecule like a block copolymer, we cannot neglect the discrete nature of the surfactant molecules, because a single block copolymer chain is already a macroscopic object. In such a case, molecular details of the surfactant may affect the macroscopic properties of the system. In most of the models mentioned so far, the directional degrees of freedom of surfactant molecules are eliminated adiabatically as was done in deriving equation (4.11). Such an elimination can be justified as long as the surfactant molecule is small and the directional degrees of freedom of surfactant molecules are equilibrated fast enough. However, when the surfactant molecule is large, directional degrees of freedom cannot be equilibrated instantaneously and may have a characteristic relaxation time comparable to that of the phase separation dynamics. In that case, one should retain the directional degrees of freedom. Moreover, a single block copolymer can induce considerable composition fluctuation by itself on the same length scale as the correlation length of the solvent due to the intramolecular structure of the block copolymer molecule. These facts suggest the necessity of a discrete treatment of surfactant molecules. Molecular detail should also be taken into account when surfactant molecules have a size asymmetry between two parts of the surfactant molecules: the surfactant molecules are adsorbed onto interfaces and give rise to spontaneous curvature of the interfaces. In order to retain such molecular details in the model, one has to treat the solvent and the surfactant in different ways. Such a model has been proposed by the present authors [38, 39, 45–47]. In this model the binary solvent is described by a continuous scalar field $X(r)$ and the surfactant is described as discrete molecules with a molecular shape. As the continuous and discrete descriptions are combined in this model, this model is named as the hybrid model.

The hybrid expression for the free energy is obtained by replacing $\psi_A(r)$ and $\psi_B(r)$ in equation (4.5) by

$$\psi_K(r) = \sum_i \psi_K^{(i)}(r) \qquad (K = A, B) \tag{4.13}$$

where $\psi_K^{(i)}(r)$ is the distribution of K monomers of the ith surfactant molecule and the summation is taken over all the surfactant molecules [38, 47]. As the function $\psi_K^{(i)}$ describes the form of the Kth subchain of the ith block copolymer chain, it can be called the form function. For a simple choice for the form function $\psi_K^{(i)}$ for a macromolecular block copolymer, one can use a Gaussian distribution of an ideal polymer chain. Then S_{int} accounts for the elastic deformation energy of the coil of the block copolymer chain.

As a surfactant molecule is composed of a pair of an A subchain and a B subchain, at least two parameters are necessary to specify the ith surfactant molecule, i.e. the position of the centre of mass r_i and the unit vector pointing from the centre of the B subchain to the centre of the A subchain denoted as $\hat{s}_i$. The description of the surfactant molecule using these two variables r_i and $\hat{s}_i$ corresponds to the dipole approximation in electromagnetism.

Then the free-energy functional can be expanded in a power series in r_i and $\hat{s}_i$ using the multipole expansion technique [38]. The resulting free-energy functional contains not only the variables r_i and $\hat{s}_i$ but also the form functions $\psi_K^{(i)}(r)$ [38]. Therefore the hybrid model can incorporate the molecular shape of the surfactant molecule (in this case the block copolymer) explicitly. Such a feature of the hybrid model is useful in simulating a surfactant molecule whose molecular shape is not simple. For example, the hybrid model can be applied to a block copolymer with a shape asymmetry between the two blocks (subchains) [48] as will be briefly mentioned in the next section.

For the equations of motion for the hybrid model, we note that the variables $r_i(t)$ and $\hat{s}_i(t)$ are not conserved variables like the field $X(r, t)$. Therefore they do not obey continuity equations like equations (4.6) and (4.7). Instead, these variables are assumed to obey the purely dissipative equations of motion:

$$\frac{\mathrm{d}}{\mathrm{d}t} r_i(t) = -L^r \frac{\partial F}{\partial r_i} \tag{4.14a}$$

$$\frac{\mathrm{d}}{\mathrm{d}t} \hat{s}_i(t) = -L^s \left[\frac{\partial F}{\partial \hat{s}_i} - \left(\frac{\partial F}{\partial \hat{s}_i} \cdot \hat{s}_i \right) \hat{s}_i \right] \tag{4.14b}$$

where L^r and L^s are mobilities of surfactant molecules. Equations (4.14*a*, *b*) are the equations of motion for a particle moving in a viscous medium. The second term on the RHS of equation (4.14*b*) comes from the constraint $|\hat{s}_i| = 1$. This hybrid model can be mapped onto a continuum model like (4.10*a–c*) by using (4.9*a–c*) and taking the small-surfactant limit [38, 39].

5. Theoretical and simulation results

In this section, we review numerical as well as theoretical results obtained by the models presented in the preceding section. For static properties of surfactant solutions, an excellent review article has already been written [16]. Thus we here concentrate on the dynamic properties focusing on the phase-separation process as an example.

In usual binary mixtures such as binary alloys and polymer blends, phase separation takes place when the binary mixture is quenched from a high-temperature disordered state to a low-temperature state where the binary mixture separates into two phases, each of which is rich in one of the two components. After a sudden temperature quench, composition fluctuations are created and grow to form domain structures in the late stage. Such a phase-separation process is roughly classified into two time regimes. One is the early stage where the amplitudes of the composition fluctuations are small so that the non-linear terms in the equations of motion can be neglected [49]. The other regime is the late stage where the composition fluctuations have fully evolved and therefore the dynamics is dominated by the non-linear effects. In this time regime, the system is divided into domains separated by interfaces, where the coarsening of domains is driven by interfacial tension [50]. The average domain size $l(t)$ grows in time as $l(t) \sim \alpha t^z$ with $z = \frac{1}{3}$ for solid alloys [51] and with $z = 1$ for fluid mixtures [52], which is called dynamical scaling [15]. One of the main interesting points is how this dynamical scaling is affected by the added surfactant.

As an example, we show in figure 10 the snapshot pictures of irregular bicontinuous structures generated using the hybrid model. In these figures, the volume fractions of A component and of B component are set to be equal. The dotted regions and the white regions correspond to A-rich domains and B-rich domains, respectively. Surfactant molecules are shown by small circles with a short line, which show the position and the direction

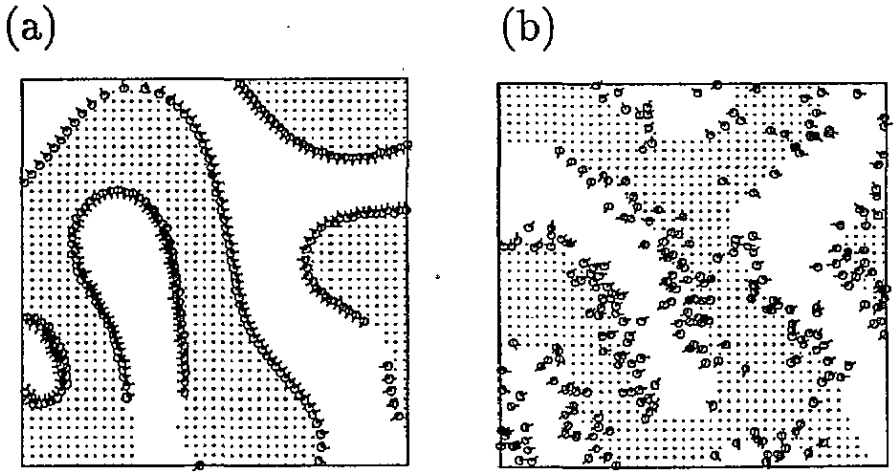

Figure 10. Snapshot pictures of irregular bicontinuous structures simulated using the hybrid model, where (a) thermal noise is neglected, and (b) thermal noise is included (see [47]).

of surfactant molecules, respectively. In figure 10(a), thermal fluctuations are neglected, while thermal fluctuation effects are taken into account in figure 10(b). One finds that the molecules are put into disorder by the thermal fluctuations. Note that the configuration shown in figure 10(b) resembles to that generated by the lattice MC simulation by Larson and co-workers (figure 8). In the model of Larson and co-workers, each lattice point is regarded as a single molecule. On the other hand, in the hybrid model, such a molecular picture for the solvent has already been averaged out and each dot in figure 10 corresponds to a number of molecules.

Using the two-dimensional hybrid model, we performed a series of simulations on the phase-separation processes from initial uniformly mixed states of the binary mixture and the surfactant [38, 39, 47]. In the following we discuss the dynamics of such phase-separation processes.

5.1. Early-stage dynamics

The dynamics of phase separation in the linear regime was investigated by Kawakatsu and Kawasaki using the hybrid model [39] and a spin model [37]. They found that the added surfactant has two opposite effects on the initial growth of the composition fluctuation of the binary solvent. The amphiphilic property enhances the phase separation, while the impurity nature (excluded volume) suppresses the phase separation. This result can intuitively be understood by using the free energy equations (4.8) and (4.11). By neglecting all the non-linear terms, the equations of motion for the field $X(\boldsymbol{r}, t)$, equations (4.6) and (4.7) combined with equation (4.8) or equation (4.11), lead to the following form:

$$\frac{\partial}{\partial t}X(\boldsymbol{r}, t) = L^{XX}\nabla^2[-cX - D\nabla^2 X] \tag{5.1}$$

where the density field ϕ and ψ in equations (4.8) and (4.11) are expanded in power series in small fluctuations around the average values and we have neglected the cross coupling terms in equation (4.7). Here, from equations (4.8) and (4.11), one finds that the parameters c and D depend on the average surfactant density $\bar{\rho}_S$ as

$$c = \frac{\chi\bar{z}}{2} - \frac{\rho_0}{\rho_0 - \bar{\rho}_S N} \qquad D = \frac{\chi a^2}{2}(1 - \gamma\bar{\rho}_S) \tag{5.2}$$

where $\gamma = 0$ for a monomeric surfactant and $\gamma > 0$ for a trimeric surfactant. The $\bar{\rho}_S$ dependence of c originates from the excluded volume effect of the surfactant molecule, while the $\bar{\rho}_S$ dependence of D is due to the amphiphilic effects. According to the discussions in the preceding section, γ is an increasing function of the surfactant molecular size. Fourier transformation of equation (5.1) leads to the following growth law for the composition fluctuation X:

$$\hat{X}(k, t) \sim \exp[\lambda(k)t] \tag{5.3}$$

where $\hat{X}(k, t)$ is the Fourier transform of $X(r, t)$ and $\lambda(k)$ is the growth rate. At $k = k_{max} \equiv (c/2D)^{1/2}$, the growth rate takes its maximum value

$$\lambda(k_{max}) = L^{XX}\frac{c^2}{4D}. \tag{5.4}$$

Combining equations (5.2) and (5.4) and neglecting the $\bar{\rho}_S$ dependence of L^{XX}, one finds that the growth rate λ is reduced for monomeric surfactant molecules, while it is increased for sufficiently large surfactant molecules [39]. Actually the enhancement of the phase separation due to the added surfactant was observed by the simulation using the two-dimensional hybrid model. In figure 11, a comparison between the results of the linear analysis and those of the computer simulation both on the hybrid model is shown. Here the surfactant density is shown by its average number density $\bar{n}_S$, which is proportional to the average surfactant density $\bar{\rho}_S$. From the data, one can confirm that an increase in the growth rate of the scattering function takes place when the surfactant is added to the binary mixture. Here the excluded volume effect of the surfactant molecule is neglected both in the simulation and in the linear analysis, and therefore the increase in the growth rate is caused by the amphiphilic nature of the surfactant molecule. On the experimental side, only the suppression of the phase separation in the early time regime was observed by Hashimoto and Izumitani [14], and the enhancement of the phase separation has not been observed experimentally. The block copolymer chain used in the experiment may be too short to detect the enhancement effects.

In the above-mentioned linear analysis, we used the free energy models where the directional degrees of freedom of surfactant molecules are already eliminated. If the relaxation of the directional degrees of freedom of the surfactant molecule is slow, the enhancement effects due to the amphiphilic nature will be reduced [39]. Such an effect may interpret the reason why the enhancement is not observed in real experiments, where the rotational relaxation of the block copolymer chains is normally very slow.

5.2. Late-stage dynamics

In the late stage of the phase separation, the system takes a domain structure and most of the surfactant molecules are adsorbed onto interfaces. As the total number of surfactant molecules is conserved, the surfactant density on interfaces is gradually increased when the coarsening of domains proceeds. The interfacial tension is a decreasing function of the surfactant density on the interface, and therefore the driving force for the coarsening is gradually decreased.

Here we show an intuitive dimensional argument [47], which predicts the slowing down of the coarsening in the late stage of the formation process of bicontinuous structures. According to this dimensional argument, the average domain size $l(t)$ as a function of time t is given by the solution of the equation

$$\frac{\mathrm{d}}{\mathrm{d}t}l(t) \sim L^{XX}(\Sigma(t))l(t)^{-2} \tag{5.5}$$

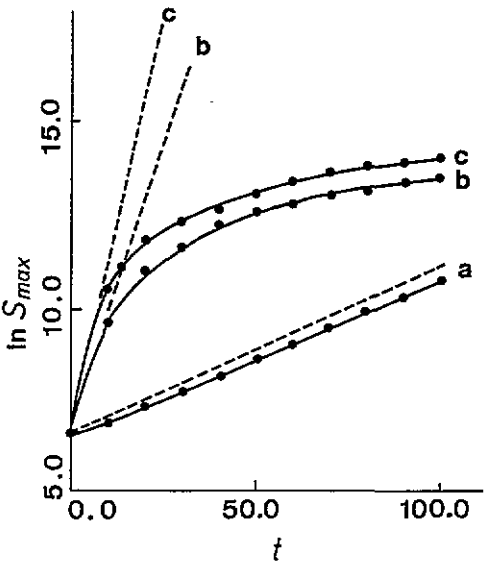

Figure 11. A comparison between the results of linear analysis (broken lines) and those of simulations of the hybrid model (solid curves) on the early-stage dynamics of the phase-separation process. The average number density of the surfactant $\bar{n}_S$ is set to be (a) 0.0, (b) 0.174 and (c) 0.347, respectively. Note that $\bar{n}_S$ is proportional to the average surfactant density $\bar{\rho}_S$ (see [39]).

where L^{XX} is the Onsager coefficients defined in equation (4.7) and $\langle\Sigma(t)\rangle$ is the interfacial tension of the surfactant-adsorbed interfaces at time t averaged over the interfaces. If the dependence of the interfacial tension on the surfactant density is known, $\langle\Sigma(t)\rangle$ is given by

$$\langle\Sigma(t)\rangle \sim \tilde{\Sigma}(l(t)/l_0) \tag{5.6}$$

where l_0 is a positive constant which corresponds to the saturation density of the surfactant on the interface. The function $\tilde{\Sigma}$ is linear in the surfactant density σ_S when $\sigma_S \ll \sigma_0$, the latter being the saturation density of the surfactant. On the other hand, when $\sigma_S \gg \sigma_0$ the interfacial tension becomes essentially constant denoted as $\tilde{\Sigma}_0$. If $\tilde{\Sigma}_0$ is almost vanishing, the phase separation is stopped when the interface is completely saturated by the surfactant. In such a case, one has the following growth laws:

$$l(t) \sim \begin{cases} t^{1/3} & (l \ll l_0) \\ \ln t & (l \geqslant l_0) \end{cases} \tag{5.7}$$

where we assumed that $\tilde{\Sigma}(\sigma_S)$ approaches $\tilde{\Sigma}_0$ exponentially as σ_S increases beyond σ_0. Therefore, the growth exponent is drastically reduced in the late stage. It should be noted that the surfactant effect is not only quantitative but also qualitative, i.e. the growth exponent z in equation (2.2) as well as the prefactor α is affected due to the added surfactant. Such a qualitative change has actually been observed by Hashimoto and Izumitani [14] (see figure 5) but it was not observed in the experiment by Roe *et al* [13]. Also the change in the growth exponent was confirmed by computer simulations by Laradji *et al* [30, 34], and by Kawakatsu *et al* [47]. In figure 12, we show the temporal changes of the characteristic length $l(t)$ obtained by Laradji *et al* for bicontinuous domain formation processes. A similar

result obtained by the computer simulation on the hybrid model by Kawakatsu *et al* but for the characteristic wave number $\bar{k}(t)$, which is roughly the inverse of $l(t)$, is shown in figure 13. A logarithmic domain growth is observed in the simulation by Laradji *et al* , which means that the domain growth is essentially frozen. On the other hand, it seems that the simulation by Kawakatsu *et al* has not yet reached the final stage where the interfacial tension is completely vanishing although a change in the growth exponent is observed.

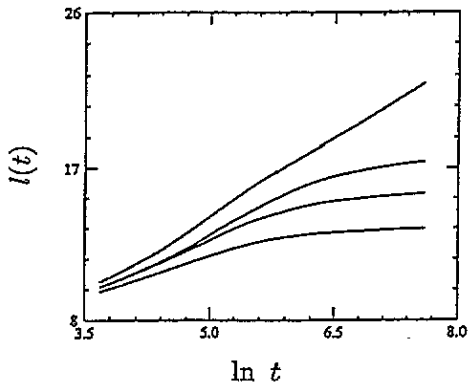

Figure 12. Temporal evolution of the characteristic length $l(t)$ for various surfactant densities calculated with the continuum model. The average surfactant density $\bar{\rho}_S$ is from top to bottom 0.1, 0.15, 0.17 and 0.2, respectively (see [34]).

A similar argument on the slowing down in the late stage has been given on micellar formation processes by Yao and Laradji [53], where they calculated the micellar size distribution function. They assumed a similar surfactant effect on the interfacial tension as was assumed for $\tilde{\Sigma}$ in equation (5.6) and showed that the micellar distribution is the same as that for the systems without surfactant. In this case the surfactant effect is only to change the time scale of the phase separation.

The functional form of the scattering function is also investigated by the hybrid model [47]. In figure 14, we show the scaled scattering function $\tilde{S}(x)$ defined by equation (2.3) obtained by the simulations on the hybrid model. Figure 14(a) shows the scaled scattering function for a simple binary mixture without surfactant, which is very similar to that obtained by the polymer experiment (figure 6(a)). Figure 14(b) shows the scaled scattering function for the case with added surfactant. Comparing figures 14(a) and 14(b), one recognizes that the scaled scattering function becomes broader when the surfactant is added. This is interpreted as follows: as the added surfactant is adsorbed onto interfaces and forms surfactant sheets on the interfaces, the interfaces undulate due to the incompressibility of the surfactant sheets as the coarsening proceeds. Such an undulation leads to the broadening of the main peak of $\tilde{S}(x)$ [47]. Such a broadening of the main peak cannot be observed in the experimental data shown in figure 6. The discrepancy may partly originate from the difference in the molecular size of the block copolymers used in the computer simulation and in the experiment. In the MD simulation by Laradji *et al* [30], they reported that no appreciable change in the scattering function was found when the surfactant is added to the binary fluid mixture. It is worthwhile to note that the surfactant molecules used in this simulation seems to be small compared to the domain size.

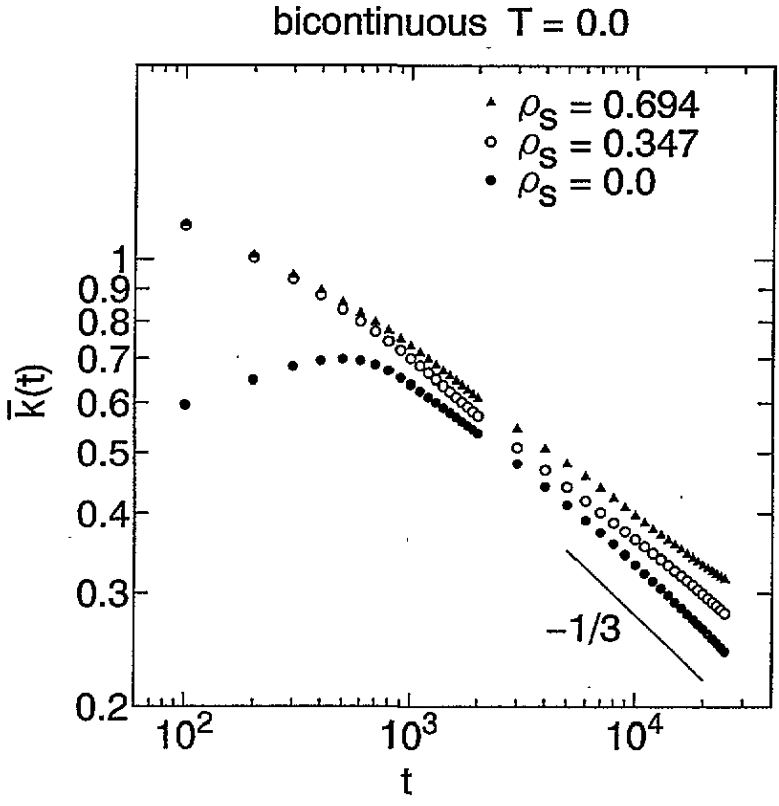

Figure 13. Temporal evolution of the characteristic wave number $\bar{k}(t)$ for the average surfactant number densities $\bar{n}_S = 0.0$, 0.347 and 0.694 calculated with the hybrid model (see [47]).

Finally we show a simulation result on the phase separation in the presence of a surfactant which has a shape asymmetry between the two blocks [48]. The shape asymmetry is introduced by changing the ratio between the χ parameters (interaction parameters with the solvent) of the two blocks, and the asymmetry is measured by the parameter $R \equiv (\chi_{AA} - \chi_{AB})/(\chi_{BB} - \chi_{AB})$. Therefore, $R = 1.0$ corresponds to the symmetric case discussed above. Here, the interactions between solvent monomers are kept unchanged. A remarkable effect of an asymmetric surfactant is the non-vanishing spontaneous curvature of the surfactant-adsorbed interface, which can lead to a morphological change of the domain structure. The temporal evolution of the characteristic wave number $\bar{k}(t)$ is shown in figure 15 for several values of R. The other parameters are the same as those used in figure 13. As the shape asymmetry is increased, the domain growth is more and more slowed down compared with the case for the symmetric surfactant. The slowing down is caused by a morphological change in the domain structure from a bicontinuous one to a micellar one, the latter has much slower growth rate than the former. Morphological changes and associating dynamics in emulsion systems are intersting problems which can be attacked by the present hybrid approach [6].

5.3. Some remarks on the hybrid model

In the above formulation and simulations, the surfactant molecule is treated as a molecule

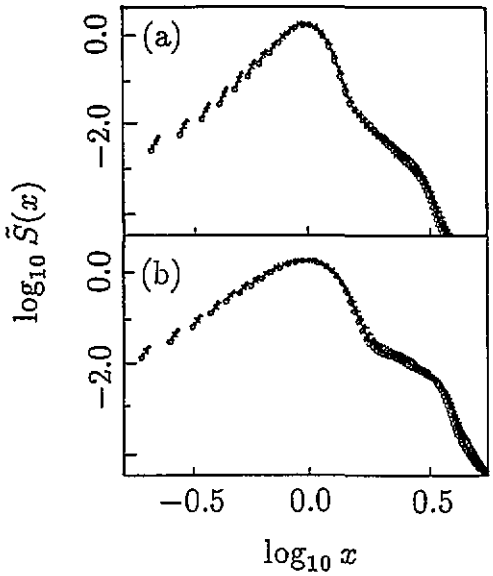

Figure 14. Scaled scattering functions $\tilde{S}(x)$ defined by equation (2.3) calculated in a computer simulation on the hybrid model. The average surfactant number densities $\bar{n}_S$ are (a) 0.0 and (b) 0.694, respectively (see [47]).

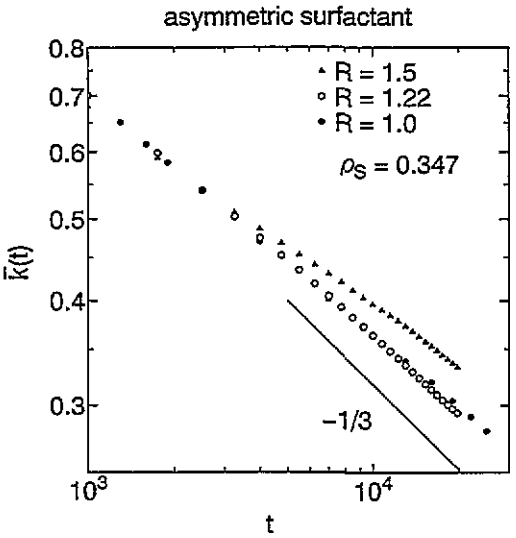

Figure 15. Temporal evolution of the characteristic wave number $\tilde{k}(t)$ calculated with the hybrid model for a system with a block copolymer (surfactant) which has an asymmetry between the two blocks. The average surfactant number density is $\bar{n}_S = 0.347$ (see [44]).

with a rigid shape and only the translational and rotational degrees of freedom are taken into account. For an actual surfactant molecule, however, not only the position and the direction but also the molecular shape may change upon association or upon adsorption onto an interface. For example, the conformation of a polymer chain is deformed due to the excluded volume effect when another chain approaches. In order to take such a deformation effects into account, one has to introduce more parameters to describe the deformation of the form function $\psi_K^{(i)}(r)$. If the undeformed shape is spherical and the shape deformation

is small, an expansion of the form function $\psi_K^{(i)}(r)$ using spherical harmonic functions will be useful. In that case, the expansion coefficients serve as the parameters describing the deformation. Such an approach will be useful in investigating the static and dynamic properties of surfactant associations like micelles, where the deformation of the molecular shape cannot be neglected.

6. Concluding remarks

Studies on dynamics of surfactant solutions have just started and there are many problems which have not yet been solved nor even attacked. The dynamical models reviewed in this article are based on many *ad hoc* assumptions especially in the way the dynamics is introduced, although the static part of the models which is expressed by the free-energy functionals is rather well understood owing to the many static works using lattice models and continuum models. Almost all of the dynamical models shown in this article adopt local dissipative dynamics just like the alloy systems. Moreover the simulations are limited to the two-dimensional case. The hydrodynamic interaction will be very important in real surfactant solutions as in the case of binary fluid mixtures and binary polymer blends [52]. Including the hydrodynamic interaction as well as extending the simulations to three-dimensional cases will be one of the important future directions.

Another future direction may be to attempt quantitative predictions on experimental systems. To accomplish this, it is helpful to derive microscopic expressions of the parameters of the coarse-grained model, the latter being much easier to simulate and analyse regarding large scale and long-time phenomena. For a quantitative comparison with experiments, the static shape and the shape deformations of the surfactant molecule should also be incorporated. These problems are interesting targets of future investigations.

Acknowledgments

We would like to thank Professors S H Chen and J-P Hansen for recommending us to contribute this article to the present journal. We also thank S H Chen, T Hashimoto, M Laradji and R G Larson for their permission to reproduce figures from their articles. T Kawakatsu would like to express his gratitude to S H Chen, T Koga and M Laradji for useful comments. Simulations on the hybrid model were performed under support by the National Laboratory for High Energy Physics and the Institute for Molecular Science and a grant-in-aid for scientific research from the Ministry of Education, Science and Culture, Japan.

References

[1] de Gennes P G 1979 *Scaling Concepts in Polymer Physics* (Ithaca, NY: Cornell University Press)
[2] Safran S A and Clark N A (ed) 1987 *Physics of Complex and Supermolecular Fluids* (New York: Wiley)
[3] Meunier J, Langevin D and Boccara N (ed) 1987 *Physics of Amphiphilic Layers* (Berlin: Springer)
[4] Davis H T, Bodet J F, Scriven L E and Miller W G 1987 *Physics of Amphiphilic Layers* ed J Meunier, D Langevin and N Boccara (Berlin: Springer)
[5] Leibler S 1989 *Statistical Mechanics of Membranes and Surfaces* vol 5, ed D Nelson, T Piran and S Weinberg (Singapore: World Scientific)
[6] Porte G 1992 *J. Phys.: Condens. Matter* 4 8649
[7] Kahlweit M, Strey R, Haase D, Kunieda H, Schmeling T, Faulhaber B, Borkovec M, Eicke H-F, Busse G, Eggers F, Funck T H, Richmann H, Magid L, Söderman O, Stilbs P, Winkler J, Dittrich A and Jahn W 1987 *J. Colloid Interface Sci.* **118** 436

[8] Jahn W and Strey R 1988 *J. Chem. Phys.* **92** 2294
[9] Teubner M and Strey R 1987 *J.Chem. Phys.* **87** 3195
[10] Chen S H, Chang S L and Strey R 1990 *J. Chem. Phys.* **93** 1907
Chen S H, Chang S L and Strey R 1990 *Prog. Colloid Polym. Sci.* **81** 30
Schubert K-V and Strey R 1991 *J. Chem. Phys.* **95** 8532
[11] Kuwahara N, Sato H and Kubota K 1993 *Phys. Rev.* **47** 1132
[12] Guenoun P, Gastaud R, Perrot F and Beysens D 1987 *Phys. Rev.* A **36** 4876
Beysens D, Guenoun P and Perrot F 1988 *Phys. Rev.* A **38** 4173
[13] Roe R J and Kuo C M 1990 *Macromolecules* **23** 4635
Park D W and Roe R J 1991 *Macromolecules* **24** 5324
[14] Hashimoto T and Izumitani T 1993 *Macromolecules* **26** 3631
Izumitani T and Hashimoto T 1994 *Macromolecules* **27** 1744
[15] Furukawa H 1985 *Adv. Phys.* **34** 703
[16] Gompper G and Schick M 1994 *Phase Transitions and Critical Phenomena* vol 16, ed C Domb and J Lebowitz (New York: Academic) at press
[17] Schulman J H and Montagne J B 1961 *Ann. NY Acad. Sci.* **92** 366
[18] Talmon Y and Prager S 1977 *Nature* **267** 333; 1978 *J. Chem. Phys.* **69** 2984; 1982 *J. Chem. Phys.* **76** 1535
[19] de Gennes P G and Taupin C 1982 *J. Phys. Chem.* **86** 2294
[20] Widom B 1984 *J. Chem. Phys.* **81** 1030
[21] Milner S T, Safran S A, Andelman D, Cates M E and Roux D 1988 *J. Physique* **49** 1065
[22] Widom B 1986 *J. Chem. Phys.* **84** 6943
[23] Dawson K A 1987 *Phys. Rev.* A **35** 1766
Dawson K A, Lipkin M D and Widom B 1988 *J. Chem. Phys.* **88** 5149
[24] Chen K, Ebner C, Jayaprakash C and Pandit R 1987 *J. Phys.: Condens. Matter* **20** L361; 1988 *Phys. Rev.* A **38** 6240
[25] Schick M and Shih W-H 1987 *Phys. Rev. Lett.* **59** 1205
[26] Gompper G and Schick M 1989 *Chem. Phys. Lett.* **163** 475
[27] Moraietz D, Chowdhury D, Vollmar S and Stauffer D 1992 *Physica* A **187** 126
[28] Larson R G, Scriven L E and Davis H T 1985 *J. Chem. Phys.* **83** 2411
Larson R G 1988 *J. Chem. Phys.* **89** 1642; 1989 *J. Chem. Phys.* **91** 2479; 1992 *J. Chem. Phys.* **96** 7904
[29] Smit B, Hilbers P A J, Esselink K, Rupert L A M, van Os N M and Schlijper A G 1991 *J. Phys. Chem.* **95** 6361
[30] Laradji M, Mouritsen O G, Toxvaerd S and Zuckermann M J 1994 *Phys. Rev.* E at press
[31] Hohenberg P C and Halperin B I 1977 *Rev. Mod. Phys.* **49** 435
[32] Chen K, Jayaprakash C, Pandit R and Wenzel W 1990 *Phys. Rev. Lett.* **65** 2736
[33] Kawasaki K and Kawakatsu T 1990 *Physica* A **164** 549
[34] Laradji M, Guo H, Grant M and Zuckermann M J 1991 *J.Phys. A: Math. Gen.* **24** L629
Laradji M, Guo H, Grant M and Zuckermann M J 1992 *J. Phys.: Condens. Matter* **4** 6715
[35] Gompper G and Kraus M 1992 *Phys. Rev.* E **47** 4289
[36] Ma S K 1976 *Modern Theory of Critical Phenomena* (New York: Benjamin)
[37] Kawakatsu T and Kawasaki K 1992 *J. Colloid Interface Sci.* **148** 23
[38] Kawakatsu T and Kawasaki K 1990 *Physica* A **167** 690
[39] Kawakatsu T and Kawasaki K 1991 *J. Colloid Interface Sci.* **145** 413, 420
[40] Helfand E and Wassermann Z R 1976 *Macromolecules* **9** 879
[41] Leibler L 1980 *Macromolecules* **13** 1602
[42] Ohta T and Kawasaki K 1986 *Macromolecules* **19** 2621
[43] Bahiana M and Oono Y 1990 *Phys. Rev.* A **41** 6763
[44] Kawakatsu T 1994 *Phys. Rev.* E submitted
[45] Kawakatsu T and Kawasaki K 1992 *Molecular Dynamics Simulations* ed F Yonezawa (Berlin: Springer)
[46] Kawakatsu T and Kawasaki K 1992 *From Phase Transitions to Chaos* ed G Györgyi, I Kondor, L Sasvári and T Tél (Singapore: World Scientific)
[47] Kawakatsu T, Kawasaki K, Furusaka M, Okabayashi H and Kanaya T 1993 *J. Chem. Phys.* **99** 8200
[48] Kawakatsu T, Kawasaki K, Furusaka M, Okabayashi H and Kanaya T 1994 *J. Chem. Phys.* submitted
[49] Cahn J W 1961 *Acta Metall.* **9** 795; 1962 *Acta Metall.* **10** 179
[50] Kawasaki K and Ohta T 1983 *Physica* A **118** 175
[51] Lifschitz I M and Slyozov V V 1961 *J. Phys. Chem. Solids* **19** 35
[52] Siggia E 1979 *Phys. Rev.* A **20** 595
[53] Yao J H and Laradji M 1993 *Phys. Rev.* E **47** 2695